25 November 2024

Anions in corrosion: Influence of polymer electrolytes on the interfacial ion transfer kinetics of Cu at Au(111) surfaces

Kira Thurman[1], Caitlyn Cannan[1], Raj Shekhar[1], Yang Zhao[1,2], Shannon Boettcher[2,1], Paul Kempler[1]

1. University of Oregon

2. University of California, Berkeley

Abstract

The corrosion kinetics of metals in the presence of polymer electrolytes—which are frequently used in devices for the electrochemical production of hydrogen, hydrocarbons, and alcohols—is convoluted by transport and ill-defined reactive interfaces which mask the fundamental reaction kinetics. Underpotential-deposited monolayers of Cu at Au(111) surfaces provide a structurally well-defined active site for interfacial ion transfer, with a fixed number of sites available for adsorption. Here, we investigate the adsorption behavior of Cu at Au(111) surfaces across a series of sulfate and sulfonate electrolytes, to understand how anion structure influences the kinetics of elementary interfacial ion-transfer reactions. The influence of anion structure is most significant at high adsorbate coverage, with similar adsorption isotherms and kinetics observed for all three molecular sulfates and sulfonates. In contrast, a suspended perfluorosulfonic acid ionomer reduced both the equilibrium coverage of Cu as well as the standard exchange rate at Au(111) at low coverages of Cu. These results suggest that electrocatalyst corrosion is inhibited for metal nanoparticles supported at polymer electrolytes due to changes in adsorbate coverage as well as suppressed kinetics for interfacial ion transfer.

https://doi.org/10.26434/chemrxiv-2024-5j7gx

Anions in corrosion: Influence of polymer electrolytes on the interfacial ion transfer kinetics of Cu at Au(111) surfaces

Kira A. Thurman,[1] Caitlyn C. Cannan,[1] Raj Shekhar,[1] Yang Zhao,[1] Shannon W. Boettcher*,[1,2] Paul A. Kempler*[1]

[1]*Department of Chemistry and Biochemistry and the Oregon Center for Electrochemistry, University of Oregon, Eugene, OR, USA*

[2] *Department of Chemical & Biomolecular Engineering and Department of Chemistry, University of California, and Energy Storage and Distributed Resources Division, Lawrence Berkeley National Laboratory, Berkeley, CA, USA*

*Correspondence: pkempler@uoregon.edu , boettcher@berkeley.edu

Abstract

The corrosion kinetics of metals in the presence of polymer electrolytes—which are frequently used in devices for the electrochemical production of hydrogen, hydrocarbons, and alcohols—is convoluted by transport and ill-defined reactive interfaces which mask the fundamental reaction kinetics. Underpotential-deposited monolayers of Cu at Au(111) surfaces provide a structurally well-defined active site for interfacial ion transfer, with a fixed number of sites available for adsorption. Here, we investigate the adsorption behavior of Cu at Au(111) surfaces across a series of sulfate and sulfonate electrolytes, to understand how anion structure influences the kinetics of elementary interfacial ion-transfer reactions. The influence of anion structure is most significant at high adsorbate coverage, with similar adsorption isotherms and kinetics observed for all three molecular sulfates and sulfonates. In contrast, a suspended perfluorosulfonic acid ionomer reduced both the equilibrium coverage of Cu as well as the standard exchange rate at Au(111) at low coverages of Cu. These results suggest that electrocatalyst corrosion is inhibited for metal nanoparticles supported at polymer electrolytes due to changes in adsorbate coverage as well as suppressed kinetics for interfacial ion transfer.

Introduction

Corrosion reactions limit the operational environments available to electrocatalysts,[1-5] conductive supports,[6, 7] semiconducting light absorbers,[8-10] and protective transparent conducting oxides used in (photo)electrochemical cells.[11, 12] These reactions are generally controlled by the transfer of ions—not electrons—through the double layer, so measurements of ion-transfer kinetics are thus critical for understanding the durability of (photo)electrochemical cells. Corroding electrode/electrolyte interfaces present many possible active surface sites, having varied free energies of adsorption and unknown activation energies for interfacial ion transfer, whereas adatoms and monolayers prepared via underpotential deposition (UPD)[13, 14] on uniform metal surfaces are limited to only a few possible sites. Because UPD reactions are inherently self-limiting, electrodes prepared from (sub)monolayer metal adatoms are well-suited for studying the fundamentals of interfacial ion transfer.

Despite the broad importance of both corrosion and electrodeposition reactions, many basic aspects of ion-transfer kinetics remain poorly understood.[15] The behavior of electrode/electrolyte interfaces is controlled by adsorbates that define the electric field. These species often bear a partial charge that is challenging to measure experimentally, but a crucial component of any robust model of the polarized interface.[16] For many transition metals where a stable, solvated, monovalent state is energetically disfavored (Zn, Ni, Fe), the exact intermediate crossing the double layer is still not known.[17, 18] However, free and adsorbed anions, as well as the organization of the solvent in the double-layer region, are believed to play a critical role in controlling ion-transfer kinetics.[19-22] An ideal system for measuring ion-transfer kinetics would include a single, well-defined active site for adsorption at an electrochemically inert metal, such as a three-fold hollow site at an Au(111) surface.

Cu is an interesting species for studying interfacial ion transfer because it exists as stable Cu^{2+} and Cu^{+} species in solution and forms UPD adlayers on many noble metal surfaces.[13] Perhaps one of the most-studied adsorption systems is the Au(111)/Cu electrode in H_2SO_4, which yields a distinct set of two, chemically reversible adsorption peaks at potentials positive of the equilibrium potential for Cu/Cu^{2+} (E_{rev}).[13, 23-25] Co-adsorbed species have been shown to disrupt the equilibrium structure of Cu UPD layers, in particular halides, but the influence of anions on the kinetics of adsorption has received less attention.[26-28] Schlaup et al. showed that introducing chloride as a co-adsorbed species in the UPD process leads to stable submonolayers which collapse at electrode potentials where Cl^- is desorbed from the Au(111)/Cu surface.[29] Coadsorbed anions do not appear to be necessary to stabilize a complete monolayer of Cu at E near E_{rev}. Cu is also the only pure metal shown to facilitate the CO_2 reduction (CO_2R) reaction with substantial activity towards multi-carbon products,[30, 31] and may be integrated in gas-diffusion-electrode microenvironments where anions exists exclusively as pendant side chains.[32-34] For this reason, we used Cu as a model system to understand how free and fixed anions influence the possibly rate-limiting step of corrosion reactions occuring in cells forming multi-carbon products from CO_2.

A series of sulfonic-acid homologs were selected to systematically compare changes to anion structure: sulfuric acid, methanesulfonic acid (MSA), triflic acid (TFMSA), and an aqueous suspension of perfluorosulfonic acid (PFSA) ionomer (Nafion® 1100). When dispersed in water, PFSA ionomers are believed to forms colloidal suspensions with tightly packed rod-like structures; the hydrophobic perfluorinated backbone aggregates to create a water-free core while the hydrophilic sulfonate groups are facing outward.[35-37] Here, we report the corrosion and deposition behavior for Cu monolayers on Au(111) in electrolytes containing only polymeric cation-conducting polymers, with no metal cations other than Cu. The interfacial ion-transfer kinetics of

Cu^{2+} on Au(111) were quantified and compared for sulfonates to determine the specific chemical factors that influence this important elementary step associated with corrosion reactions.

Methods

Chemicals: Deionized water having a resistivity >18.2 MΩ-cm, DI H_2O, was obtained from a laboratory water purification system (Barnstead Ultrapure). Sulfuric acid (H_2SO_4 96%, TraceMetal Grade) was obtained from Fisher Chemical, methanesulfonic acid (CH_3SO_3H, 70.6%) was obtained from Alfa Aesar, and triflic acid (CF_3SO_3H, 99% extra pure) was obtained from Acros Organics. A 10% aqueous suspension of perfluorosulfonic acid, PFSA, ionomer (10 w%) was obtained from the Fuel Cell Store. Cuprous oxide was obtained from Acros Organics (ACS reagent) and was used as a consistent source of Cu^{2+} for all other anions present in supporting electrolytes and was added in concentrations well below the solubility limit of Cu^{2+}(aq). Typical Cu^{2+} containing electrolytes were prepared by dissolving CuO (1 mM Cu equivalent) in 10 mM acid such that the final [Cu^{2+}] was 1 mM and the final pH was ~2.1.

Electrodes: Au(111) surfaces were prepared from thermally evaporated films of Au on titanium-coated glass substrates (see **Supporting Information**).[38, 39] Glass slides were cleaned in an O_2 plasma and transferred to a thin-film deposition system (Angstrom Engineering) with a base pressure of 10^{-6} torr. Ti was deposited via electron-beam evaporation at 0.2 Å s^{-1} to a nominal thickness of 17 nm followed by Au deposited via thermal evaporation at 0.2 Å s^{-1} to 0.5Å s^{-1} to a nominal thickness of 200 nm; a shadow mask defined the working area of the electrode surface. Electrodes were carefully annealed in a butane gas flame and cooled under Ar immediately before transferring the surface to the cell environment.

Electrochemical characterization: All glassware was cleaned in sulfuric acid with a persulfate-based oxidizing agent (Alnochromix) and boiled and washed in deionized water at least three times before use. A Pt wire (Alfa Aesar 99.95%) served as the counter electrode and a reference electrode, Cu/Cu^{2+}(aq, 10 mM), was prepared from a clean Cu wire (Alfa Aesar, 99.999% metals basis) in a supporting electrolyte identical to the working electrochemical cell but maintained behind a microporous glass frit. All potentials are reported versus the equilibrium potential for Cu deposition from Cu^{2+}(aq), E_{rev}. Solutions were purged with ultra-high-purity Ar (99.999%) and maintained under a blanket of flowing Ar gas throughout the experiments. All Cu-containing solutions were prepared by dissolving 1 mM CuO in 10 mM H**A** where **A** was HSO_4^- (HSA), $CH_3SO_3^-$ (MSA), $CF_3SO_3^-$ (TFMSA), except for the polymer solution which was prepared as a 10 meq suspension of perfluorosulfonic acid ionomer electrolyte (PFSA). More-concentrated suspensions of PFSA could not be purged with Ar due to the generation of persistent foams. Surfaces were conditioned by sweeping the potential at 20 mV s^{-1} in 1 mM Cu^{2+} dissolved from CuO in 10 mM H_2SO_4 from 0.95 to 0 V vs E_{rev} until a steady electrochemical response was reached (4-10 cycles).

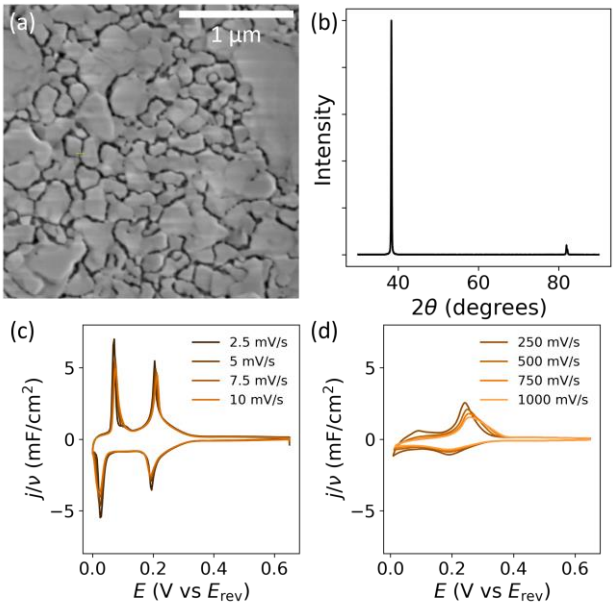

Figure 1: Physical and electrochemical characterization of Au(111) surfaces. **(a)** Scanning electron micrograph of annealed Au surface. **(b)** X-ray diffraction pattern from the Au surface collected at normal incidence. **(c)** Representative voltammetry of annealed Au(111) electrodes in 1 mM CuO, 10 mM H_2SO_4 at slow scan rates (ν = 2.5, 5, 7.5, 10 mV s^{-1}) **(d)** Representative voltammetry of annealed Au electrodes in 1 mM CuO, 10 mM H_2SO_4 at fast scan rates (ν = 250, 500, 750, 1000 mV s^{-1})

Results

Scanning-electron microscopy of the annealed Au electrode surfaces revealed the presence of terraces ranging from 10s to 100s of nm in width (**Figure 1a**) and surface X-ray

diffraction displayed only the diffraction peaks expected from an Au(111) surface (**Figure 1b**). All Au(111) electrodes were first characterized in 1 mM Cu^{2+} (aq), 10 mM SO_4^{2-}(aq) to verify the consistency of the annealing process. Whereas as-deposited Au films yielded multiple, broad cathodic peaks (**Figure S1**), the voltammetric response of annealed Au surfaces displayed a single pair of sharp cathodic peaks at 0.19 and 0.03 V vs. E_{rev} (v = 2.5 mV s^{-1}) with charge-balanced anodic peaks at 0.07 and 0.20 V, respectively, characteristic of UPD of Cu on Au(111) (**Figure 1c**).

Because our focus is on adsorptive processes, voltammetry is presented as current density normalized to scan rate, j/v, as a function of potential, E, which as the units of areal capacitance The cathodic charge passed was integrated from E = 0.0–0.6 V vs. E_{rev} and compared against the theoretical charge for complete adsorption of Cu^{2+} onto the Au(111) surface (Q_{Cu}^{*} = –0.44 mC cm^{-2}) to estimate the Cu coverage, θ_{Cu} (**Figure S2a**, Equation 1)

$$\theta_{\mathrm{Cu}}(E) = \frac{1}{Q_{\mathrm{Cu}}^{*}} \int_{0.360}^{E} j/v \, dE \qquad \textbf{(1)}$$

θ_{Cu}(0.0 V) was >0.9 for $v \leq$ 25 mV s^{-1} and then decreased steadily with increasing v to < 0.45 at 1000 mV s^{-1} (**Figure 1d)**. At increased scan rates (v > 100 mV s^{-1}) a single quasi-reversible wave was observed, with $E_{1/2}$ = 0.22(1) V for all v. Based on characterization via scanning tunneling microscopy,[27, 40, 41] *in-situ* X-ray diffraction,[42] and X-ray absorption spectroscopy[23, 24] of similar surfaces, the more positive adsorption peak was assigned to the UPD of Cu^{2+} along with SO_4^{2-} and the second peak was ascribed to the formation of a nearly complete monolayer of Cu on the Au(111) surface.

The Au(111) electrodes cleaned in DI H_2O and transferred to a cell containing 1 mM CuO, 10 meq PSFA produced a voltammetric response that was distinct from electrodes in H_2SO_4 electrolyte at all scan rates (**Figure 2a**). Characterization of the electrolyte using dynamic light scattering suggested that it was described by a suspension of ~100 nm dispersed colloidal ionomer, which was acidic enough to dissolve the solid CuO (**Figure S3**). No scattering particles were observed for CuO dissolved in any other electrolytes tested in this work. At ν = 5 mV s^{-1}, the onset of Cu adsorption occurred at E_{rev} < 0.3 V with a minor cathodic peak at ~0.15 V and a larger cathodic wave that could not be resolved prior to bulk Cu deposition. A sharp and well-defined anodic peak was evident for ν = 5–25 mV s^{-1}, with E_p shifting positively from 0.17–0.22 V. For ν = 50–1000 mV s^{-1} a single anodic and cathodic wave were observed, with a peak capacitance and integrated area that quickly decreased with increasing ν. The anodic peak potential, E_{pa}, shifted negatively by 0.040 V from 0.192 to 0.152 V, while the cathodic peak potential, E_{pc}, shifted positively by > 0.130 V from 0.232 to 0.368 V. Less Cu was adsorbed onto the Au(111) surface from PFSA electrolytes compared to H_2SO_4 electrolytes and the adsorption kinetics were more-strongly affected by increasing ν at both low and high coverages (**Figure 2b**). At slow scan rates (ν = 2.5 mV s^{-1}), an incomplete monolayer was formed (Q_{ad} ~ 0.3 mC cm^{-2}) and at the fastest scan rates Q_{ad} < 0.041 mC cm^{-2}, corresponding to θ_{Cu} < 0.10 (**Figure 2b, Figure S2d**).

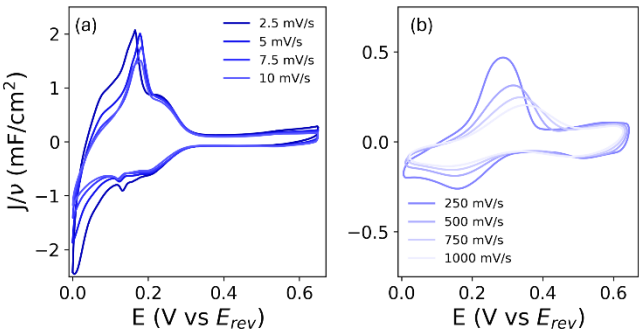

Figure 2: Cu UPD in aqueous PFSA electrolyte . **(a)** Voltammetry of annealed Au(111) electrodes in 1 mM CuO, 10 meq PFSA at slow scan rates (ν = 2.5, 5, 7.5, 10 mV s^{-1}) **(b)** Voltammetry in 1 mM CuO, 10 mM H_2SO_4 at fast scan rates (ν = 250, 500, 750, 1000 mV s^{-1})

To understand the differences caused by the polymeric nature of PFSA and those resulting from chemical differences between sulfonate and sulfate anions, we measured the UPD and corrosion behavior of Cu in two additional electrolytes (**Figure 3**). Methane sulfonic acid (MSA), CH_3SO_3H, and triflic acid (TFMSA), CF_3SO_3H, were selected as representative hydrocarbon and fluorocarbon sulfonate anions. The voltammetry of Au(111) in 1 mM CuO, 10 mM MSA is presented in **Figure 3a**, where at ν = 2.5–20 mV s^{-1} sharp cathodic peak was observed at E_{pc} = 0.017–0.075 V with a corresponding anodic peak at E = 0.15–0.24 V. Q_{ad} ~ 0.4 µC cm^{-2} at ν = 2.5 mV s^{-1} (**Figure S2b**) suggesting that nearly a complete Cu monolayer could be formed from sulfonate solutions at sufficiently slow ν. At increased ν (75–1000 mV s^{-1}) only a single, broad cathodic wave at E_{pc} = 0.23–0.17 V was connected to an anodic peak, which shifted positively with increasing scan rates from E_{pa} = 0.24–0.35 V. The voltammetric response was similar in both MSA and TFMSA, particularly at high ν. The Au(111) in 1 mM CuO and 10 mM TFMSA yielded a single desorption peak at all ν, but a sharp adsorption peak was observed for $\nu \leq 25$ mV s^{-1}. For both MSA and TFMSA electrolytes, Q_{ad} decreased with increasing ν, with a maximum of 0.16 and 0.14 mC cm^{-2} at ν = 1000 mV s^{-1} (θ_{Cu} ~ 1/3) (**Figure S2b,c**).

At positive E (corresponding to low θ_{Cu}), the onset of Cu adsorption and the tail end of Cu desorption were similar (E ~ 0.3 V) across all four electrolytes despite the varied j-E behavior at

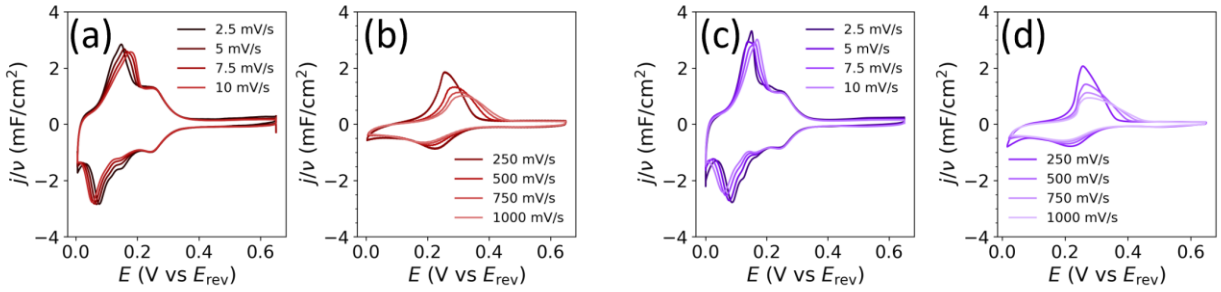

Figure 3: Cu UPD in representative molecular sulfonate electrolytes. Scan rate dependence (**a**) 2.5, 5, 7.5, 10 mV s^{-1} and **(b)** 250, 500, 750, and 1000 mV s^{-1} for Cu adsorption on Au(111) electrodes in 1 mM CuO, 10 mM MSA **(c,d)** Scan rate dependence in 1 mM CuO, 10 mM TFMSA.

increasing θ_{Cu} (**Figure 4**). At low scan rates, the adsorption and desorption capacitance were nearly symmetric in E and invariant with v, indicating reversible kinetics for Cu adsorption and desorption. The broad adsorption wave in this potential region has previously been assigned to "random" adsorption of Cu onto the Au(111) surface.[25] We interpret the similar peak character for the four anions to suggest that at low coverages the adsorption sites for Cu at Au(111) are invariant with the supporting anion.

To characterize the adsorption behavior of anions present in Cu adsorption/desorption experiments, we collected voltammetry for Au(111) electrodes in acids that were free of CuO and at a comparable ionic strength (**Figure S4**). Au(111) exhibited C_{dl} > 80 μC cm^{-2} for all E in 10 mM H_2SO_4 and showed pseudocapacitive peaks at E = 0.24 and 0.48 V vs E_{rev} (**Figure S4a**). In contrast, the PFSA electrolyte yielded a nearly constant C_{dl} ~ 30 μC cm^{-2} until the onset of oxidation of the Au(111) surface at E > 0.5 V (**Figure S4d**). Au(111) surfaces in H_2SO_4 were stable at E < 1.0 V with a small set of peaks at 0.84 and 0.88 V previously attributed to an ordered-to-disordered phase transition of adsorbed HSO_4^-.[43] Voltammetry of Au(111) surfaces in aqueous

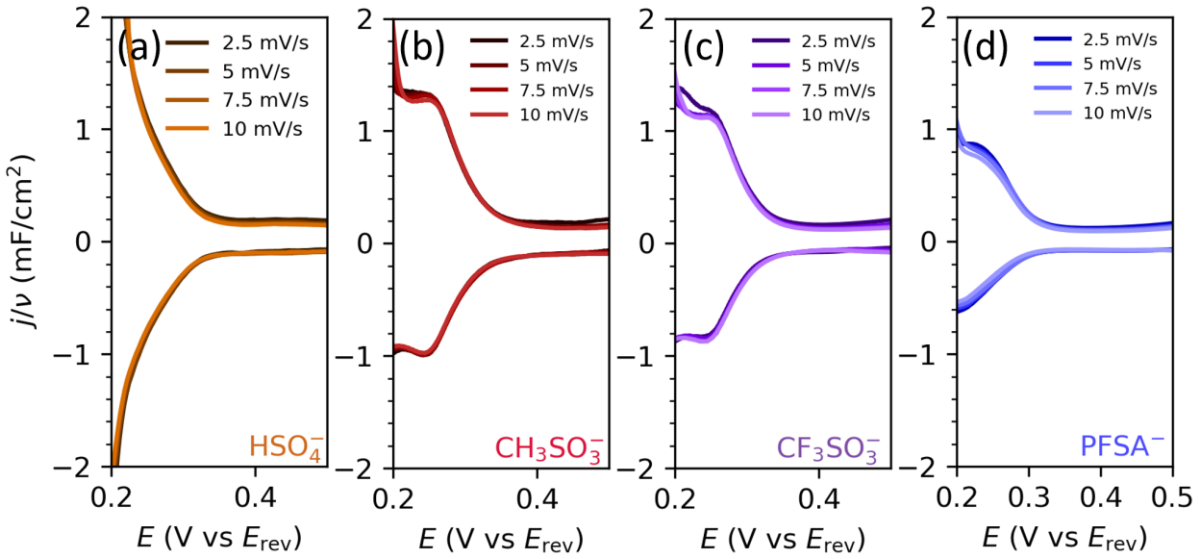

Figure 4: Comparison of adsorption onset for sulfate and sulfonate electrolytes. Kinetically reversible adsorption behavior was observed for Cu^{2+} in **(a)** H_2SO_4, **(b)** MSA, **(c)** TFMSA, and **(d)** PFSA, for scan rates v = 2.5–10 mV s^{-1}.

10 mM MSA or 10 mM TFMSA did not show prominent current peaks indicative of specific adsorption, with C_{dl} between 50 and 125 μC cm^{-2} for MSA and between 30 and 85 μC cm^{-2} for TFMSA (**Figure S4b,c**). The Au(111) surface in the presence of the sulfonate anions, or possibly the anions themselves, showed a reduced oxidative stability relative to sulfate, with irreversible faradaic currents observed for $E > 0.8$ V (**Figure S5**).

Discussion

Cu^{2+}(aq) prepared from CuO dissolved in an aqueous suspension of $PFSA^-$ anions facilitated direct measurements of the potential dependence of θ_{Cu}, as well as Cu^{2+} adsorption kinetics, without competing transport limitations through solid-polymer electrolytes and *without the competing influence of other anions*. The equilibrium adsorption behavior of Cu at Au(111) in the presence of PFSA (**Figure 2a**) is substantially different from behavior observed in the presence of HSO_4^- (**Figure 1a**). Cu adsorption from PFSA electrolytes led to lower θ_{Cu} and impeded the formation of an ordered Cu monolayer despite yielding similar θ_{Cu}-E behavior at low θ_{Cu} (**Figure 4**).

These data highlight the role of charge-balancing anions in enabling increased coverage of charged surface intermediates. Co-adsorbed sulfate is associated with higher θ_{Cu} at more-positive potentials in comparison to singly-charged MSA and TFMSA (**Figure 3a,c**). Despite similarities in structure, sulfonate anion groups are expected to interact differently with multivalent corrosion products such as Cu^{2+}. Moreover, polymer chains with PFSA acid groups have been observed via electrochemical quartz-crystal microbalance and atomic-force microscopy to specifically adsorb to the Au(111) surface, and can thus compete with Cu for adsorption sites.[44] Uncharged polymer backbones may suppress interfacial ion transfer and reduce the surface coverage of Cu^{2+} via direct

competition for adsorption sites or also by displacing charge-balancing anions at the surface or within the double layer.[45] The absence of the typical voltage-driven surface phase transition observed for $CuSO_4$ electrolytes at Au(111) at $v \geq 250$ mV s^{-1} (**Figure 1c**), and qualitatively similar voltammetry across all three anions, indicates that the voltametric response at fast scan rates was governed by the adsorption of Cu^{2+} only (**Figures 2, 3**).

Adsorption of Cu at low θ_{Cu} is quasi-reversible and allowed the direct measurement of Cu interfacial ion-transfer kinetics as a function of the anion environment. At low θ_{Cu} (E > 0.3 and θ_{Cu} < 0.05), the equilibrium adsorption behavior was similar for all sulfonate electrolytes (**Figure 4**), consistent with mechanism described by Equation 4 which is independent of the anion identity (**Equation 2**).

$$Cu^{2+}(aq) + * \rightleftarrows Cu^{*} + 2e^{-} \qquad \textbf{(2)}$$

The distinct adsorption behavior for Cu^{2+} in the presence of sulfate as compared to sulfonates converged to a qualitatively similar set of peaks at the fastest scan rates, which was commensurate with a decrease in the maximum coverage to θ_{Cu} < 0.2 (**Figures 1, 3, S2**). This is consistent with a model for UPD where ordered adlayers of Cu and supporting anions are necessary to stabilize the excess surface charge associated with θ_{Cu} > 0.2 when $E >> E_{rev}$.

The exchange rate for Cu adsorption and desorption was estimated using a method of analysis developed by Kuo et al. for quantifying the rates of proton adsorption onto Pt(111).[46] Cu adsorption rates were estimated from the current during the cathodic sweep from E = 0.36 V to 0.2 V, which ensured that Cu adsorption primarily occurs on isolated Au(111) adsorption sites, with the further assumption that Cu^{2+} completely transferred through the double layer to coordinate with the Au surface. Although *in-situ* x-ray absorption near-edge structure measurements

(XANES) suggest the oxidation state of Cu at these potentials is approximately +1,[47] the total integrated charge (~–440 μC cm^{-2}) is consistent with complete transfer of Cu^{2+} through the electrochemical double layer (μC cm^{-2}).[13]

A baseline correction to the current is applied using the capacitance at 0.36 V vs E_{rev} and θ_{Cu} is then estimated from the remaining integrated charge normalized to Q_{Cu}^{*}.[13] The apparent interfacial ion transfer rate (k_{app}) was calculated by **Equation 3**

$$k_{app} = \frac{j(E)}{|Q_{Cu}^{*}|} \quad (3)$$

where j is the current density corrected for double layer charging in the absence of Cu^{2+}, (**Figure 5**). We fit interfacial ion-transfer kinetics to a Butler-Volmer-type equation (Equation 2) where the driving force, ξ ($E - E_{eq}$), is assumed to vary with the difference in the applied electrode potential from the experimentally observed equilibrium potential (**Equation 4**)

$$k_{app} = k_0\sqrt{\theta_{Cu}(1-\theta_{Cu})}\left[\exp\left(\frac{\alpha e\xi}{k_bT}\right) - \exp\left(-\frac{(1-\alpha)e\xi}{k_bT}\right)\right] \quad (4)$$

where α, e, k_b, T, and k_0 are the transfer coefficient, elementary charge, Boltzmann constant, temperature, and standard exchange rate. The E_{eq} are measured at a sweep rate of 7.5 mV s^{-1}, sufficiently slow to give a response that well approximates the equilibrium response, that is, the collected j/v data is no longer a strong function v. The experimental data were fit to **(4)** using a non-linear least-squares algorithm to determine k_0, assuming α = 0.5.[46, 48]

When Cu occupied 5% of the available surface sites, k_0 for Cu^{2+} interfacial ion transfer is 0.25(6) s^{-1} in the presence of HSO_4^- and was 0.19(9) s^{-1} and 0.22(7) s^{-1} for Cu^{2+} in the presence of MSA and TFMSA, respectively (**Figure 5**). Thus, despite the significant changes to the adsorption behavior in the high θ_{Cu} limit, differences in the identity of non-polymer sulfonate anions had no significant influence on the interfacial ion-transfer kinetics at low θ_{Cu}. However, when PFSA

served as the supporting anion, the standard exchange rate is reduced by approximately one order of magnitude (k_0 = 0.016(5) s^{-1}). This may be related to a lower number of available surface sites for adsorption (**Figure 2**) and/or a greater free energy barrier for reorganization during interfacial ion transfer due to the additional steric and rotational constraints on polyanions. The consequence of this change should be lower rates of Cu corrosion into PFSA electrolytes, which is consistent with studies finding reduced corrosion rates of kinetically stable catalysts such as IrO_2 when operated in a membrane-electrode assembly as compared to conventional acid electrolytes.[49]

The dependence of k_0 on θ_{Cu} is presented in **Figure 6**. In contrast with previous measurements for proton adsorption at Pt(111), which found that k_0 was constant after correcting for proton coverage (and thus electrode potential), we find that an uncorrected k_0 is approximately constant for θ_{Cu} < 0.1 in H_2SO_4 electrolytes whereas k_0 is weakly dependent on θ_{Cu} for both MSA and TFMSA. The standard exchange rate, k_0, can be multiplied by the available adsorption sites and the formal charge on dissolved Cu^{2+} to be expressed as an equivalent exchange current density, j_0. This value facilitates comparison to other reactions involving interfacial ion transfer. The observed j_0 for the molecular sulfate and sulfonates is 0.11 mA cm^{-2} (**Figure 5**) which is only

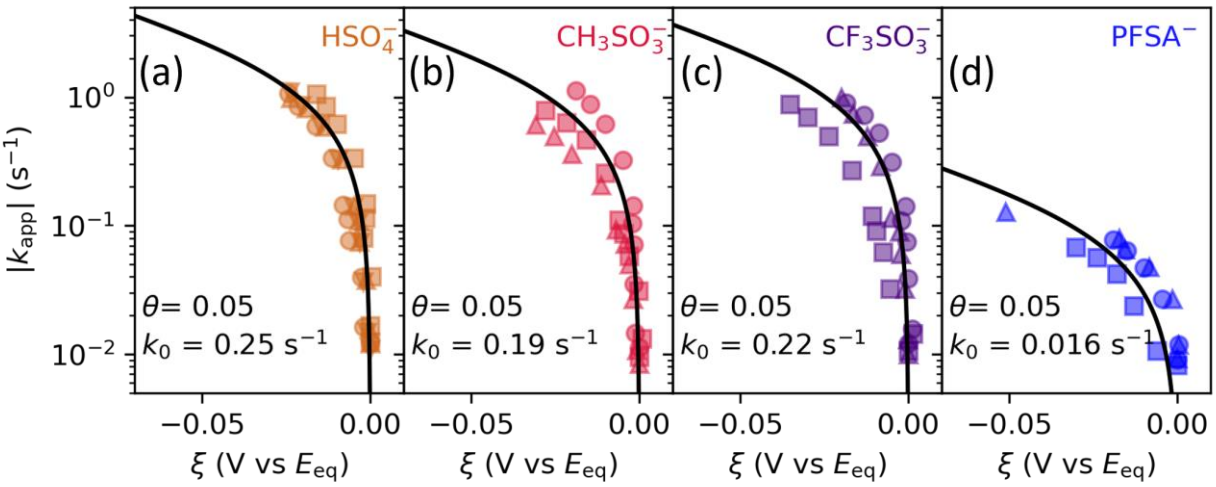

Figure 5. Interfacial Cu transfer apparent interfacial ion transfer rate vs driving force at 5% coverage of Cu on an Au(111) surface in 1 mM CuO in **(a)** 10 mM H_2SO_4, **(b)** 10 mM MSA **(c)** 10 mM TFMSA and **(d)** 10 meq $PFSA^-$ ionomer electrolyte. Data were fit with **Equation 4** (solid black line) to calculate k_0.

slightly lower than the j_0 (0.35 mA cm^{-2}) reported for the electrocrystallization of Cu from sulfate electrolytes at Cu(111) and is consistent with a kinetic model where interfacial ion transfer is the rate determining step for metal deposition.[50]

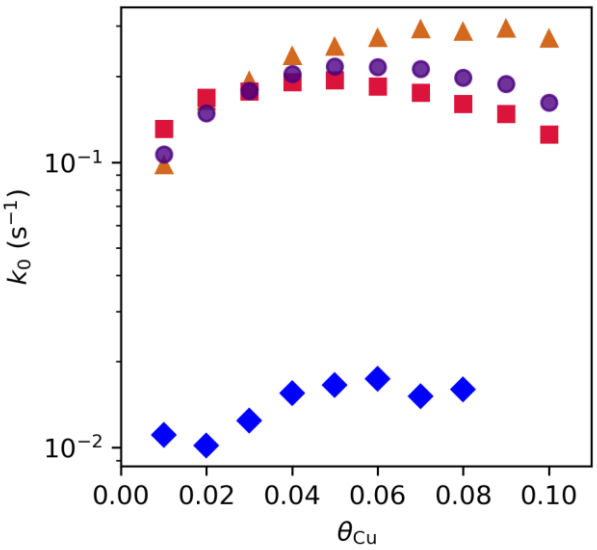

Figure 6: Coverage dependence for k_0 for various supporting anions, H_2SO_4 (orange triangles), MSA (red squares), TFMSA (purple circles), PFSA (blue diamonds).

Due to the size of Au(111) terraces available for adsorption, we expect these data to represent the rate associated with ion transfer to isolated terrace sites, but different electrode kinetics may be expected at the edges of actively growing Cu(111) terraces.[38] The j_0 values measured for H adsorption at Pt(111) from H_3O^+ (253 ± 75 mA cm^{-2}) and also H_2O/OH^- (2.2 ± 0.3 mA cm^{-2}) highlight the substantial difference in kinetics between proton-coupled adsorption reactions and interfacial ion-transfer of multivalent transition metals.[46] Similar j_0 = 0.39 and 0.19 mA cm^{-2} have been reported for divalent Pb^{2+}/Pb and Cd^{2+}/Cd, respectively and these cations may serve in future studies on the influence of cation identity underpotential deposition kinetics at Au(111).[51] For monovalent ions, such as Ag/Ag^+ on gold-supported Ag nanoclusters, much larger j_0 (~50 mA cm^{-2}) were found at room temperature, consisting of a lower solvation/desolvation barrier.[52] However, quantitative comparison of j_0 for polycrystalline systems is difficult because the exact number of deposition and stripping sites cannot be directly determined. Future studies comparing interfacial ion transfer exchange rates as a function of formal charge can address this gap.

Conclusions

Cu^{2+} adsorption at Au(111) was chosen as a model system for studying the effects of molecular and polymeric anions on the kinetics for interfacial ion transfer, an elementary step associated with corrosion, and the reverse reaction, electrodeposition. We find that simple changes to the structure of the anion have a substantial difference on the equilibrium adsorption voltammetry of Cu, with the stabilization of ordered adlayers at positive potentials disrupted by the substitution of the $–OH^-$ on sulfate with either a $–CH_3$ or $–CF_3$. The interfacial ion-transfer kinetics of Cu adsorption were quantified in the limit of random adsorption and found to be independent of anion identity for molecular sulfate and sulfonates. Suspended perfluorosulfonic acid ionomer electrolytes inhibited the equilibrium coverage of Cu at Au(111) and also suppressed interfacial ion transfer kinetics by roughly an order of magnitude. This indicates that the direct consequence of an electrochemical double layer containing only polymer-tethered anions is to diminish the standard rate constant for metal corrosion, which could contribute to the improved durability of electrocatalysts operated polymer electrolyte membrane devices.

Acknowledgments

This material is based on work performed by the Liquid Sunlight Alliance, which is supported by the U.S. Department of Energy, Office of Science, Office of Basic Energy Sciences, Fuels from Sunlight Hub under Award Number DE-SC0021266. We thank Aaron Kaufman, Jason Prachar, and Fuding Lin for assistance with preparation of Au thin films and Nicole Sagui for assistance with dynamic light scattering measurements.

References

(1) Cherevko, S. Stability and dissolution of electrocatalysts: Building the bridge between model and “real world” systems. *Curr. Opin. Electrochem.* **2018**, *8*, 118-125.
(2) Bae, J. H.; Brocenschi, R. F.; Kisslinger, K.; Xin, H. L.; Mirkin, M. V. Dissolution of Pt during oxygen reduction reaction produces Pt nanoparticles. *Anal. Chem.* **2017**, *89* (23), 12618-12621.
(3) Zhang, X.; Li, J.; Li, Y.-Y.; Jung, Y.; Kuang, Y.; Zhu, G.; Liang, Y.; Dai, H. Selective and high current CO2 electro-reduction to multicarbon products in near-neutral KCl electrolytes. *JACS* **2021**, *143* (8), 3245-3255.
(4) Watkins, N. B.; Wu, Y.; Nie, W.; Peters, J. C.; Agapie, T. In situ deposited polyaromatic layer generates robust copper catalyst for selective electrochemical CO2 reduction at variable pH. *ACS Energy Lett.* **2022**, *8* (1), 189-195.
(5) de Jesus Gálvez-Vázquez, M.; Moreno-García, P.; Xu, H.; Hou, Y.; Hu, H.; Montiel, I. Z.; Rudnev, A. V.; Alinejad, S.; Grozovski, V.; Wiley, B. J. Environment matters: CO2RR electrocatalyst performance testing in a gas-fed zero-gap electrolyzer. *ACS Catal.* **2020**, *10* (21), 13096-13108.
(6) Liu, C.; Carmo, M.; Bender, G.; Everwand, A.; Lickert, T.; Young, J. L.; Smolinka, T.; Stolten, D.; Lehnert, W. Performance enhancement of PEM electrolyzers through iridium-coated titanium porous transport layers. *Electrochem. Comm.* **2018**, *97*, 96-99.
(7) Meyers, J. P.; Darling, R. M. Model of carbon corrosion in PEM fuel cells. *J. Electrochem. Soc.* **2006**, *153* (8), A1432.
(8) Gerischer, H. The impact of semiconductors on the concepts of electrochemistry. *Electrochim. acta* **1990**, *35* (11-12), 1677-1699.
(9) Hu, S.; Lewis, N. S.; Ager, J. W.; Yang, J.; McKone, J. R.; Strandwitz, N. C. Thin-film materials for the protection of semiconducting photoelectrodes in solar-fuel generators. *J Phys. Chem. C* **2015**, *119* (43), 24201-24228.
(10) Ben-Naim, M.; Britto, R. J.; Aldridge, C. W.; Mow, R.; Steiner, M. A.; Nielander, A. C.; King, L. A.; Friedman, D. J.; Deutsch, T. G.; Young, J. L. Addressing the stability gap in photoelectrochemistry: molybdenum disulfide protective catalysts for tandem III–V unassisted solar water splitting. *ACS Energy Lett.* **2020**, *5* (8), 2631-2640.
(11) Buabthong, P.; Ifkovits, Z. P.; Kempler, P. A.; Chen, Y.; Nunez, P. D.; Brunschwig, B. S.; Papadantonakis, K. M.; Lewis, N. S. Failure modes of protection layers produced by atomic layer deposition of amorphous TiO 2 on GaAs anodes. *Energy Environ. Sci.* **2020**, *13* (11), 4269-4279.
(12) Dong, Y.; Abbasi, M.; Meng, J.; German, L.; Carlos, C.; Li, J.; Zhang, Z.; Morgan, D.; Hwang, J.; Wang, X. Substantial lifetime enhancement for Si-based photoanodes enabled by amorphous TiO2 coating with improved stoichiometry. *Nat. Commun.* **2023**, *14* (1), 1865.
(13) Herrero, E.; Buller, L. J.; Abruna, H. D. Underpotential deposition at single crystal surfaces of Au, Pt, Ag and other materials. *Chem. Rev.* **2001**, *101* (7), 1897-1930. DOI: 10.1021/cr9600363.
(14) Schmickler, W. *Interfacial electrochemistry*; Oxford University Press, 1996.
(15) Gileadi, E. Problems in interfacial electrochemistry that have been swept under the carpet. *J. Solid State Electrochem.* **2011**, *15*, 1359-1371.
(16) Guidelli, R.; Schmickler, W. Electrosorption valency and partial charge transfer. In *Modern Aspects of Electrochemistry*, Springer, 2005; pp 303-371.

(17) Pinto, L. M.; Quaino, P.; Santos, E.; Schmickler, W. On the electrochemical deposition and dissolution of divalent metal ions. *Chemphyschem* **2014**, *15* (1), 132-138.
(18) Gileadi, E. The enigma of metal deposition. *J. Electroanal. Chem.* **2011**, *660* (2), 247-253.
(19) Saraby-Reintjes, A.; Fleischmann, M. Kinetics of electrodeposition of nickel from watts baths. *Electrochim. acta* **1984**, *29* (4), 557-566.
(20) El Miligy, A.; Hilbert, F.; Lorenz, W. Kinetics of Iron Deposition on a Rotating Platinum Disk Electrode. *J Electrochem Soc* **1973**, *120* (2), 247.
(21) Pecina, O.; Schmickler, W. On the dynamics of electrochemical ion-transfer reactions. *J Electroanal Chem* **1998**, *450* (2), 303-311.
(22) Wang, F.; Borodin, O.; Gao, T.; Fan, X.; Sun, W.; Han, F.; Faraone, A.; Dura, J. A.; Xu, K.; Wang, C. Highly reversible zinc metal anode for aqueous batteries. *Nat. Mater.* **2018**, *17* (6), 543-549.
(23) Melroy, O. R.; Samant, M.; Borges, G.; Gordon, J.; Blum, L.; White, J.; Albarelli, M.; McMillan, M.; Abruna, H. In-plane structure of underpotentially deposited copper on gold (111) determined by surface EXAFS. *Langmuir* **1988**, *4* (3), 728-732.
(24) Herrero, E.; Glazier, S.; Abruna, H. D. X-ray and electrochemical studies of Cu UPD on Au (111) single-crystal electrodes in the presence of bromide. *J. Phys. Chem. B* **1998**, *102* (49), 9825-9833.
(25) Holzle, M. H.; Retter, U.; Kolb, D. M. The Kinetics of Structural-Changes in Cu Adlayers on Au(111). *J. Electroanal. Chem.* **1994**, *371* (1-2), 101-109. DOI: 10.1016/0022-0728(93)03235-H.
(26) Xue, S.; Garlyyev, B.; Auer, A.; Kunze-Liebhäuser, J.; Bandarenka, A. S. How the nature of the alkali metal cations influences the double-layer capacitance of Cu, Au, and Pt single-crystal electrodes. *J Phys. Chem. C* **2020**, *124* (23), 12442-12447.
(27) Matsumoto, H.; Inukai, J.; Ito, M. Structures of copper and halides on Pt (111), Pt (100) and Au (111) electrode surfaces studied by in-situ scanning tunneling microscopy. *J Electroanal Chem* **1994**, *379* (1-2), 223-231.
(28) Nagy, G.; Wandlowski, T. Double layer properties of Au (111)/H2SO4 (Cl)+ Cu2+ from distance tunneling spectroscopy. *Langmuir* **2003**, *19* (24), 10271-10280.
(29) Schlaup, C.; Horch, S.; Chorkendorff, I. On the stability of copper overlayers on Au (1 1 1) and Au (1 0 0) electrodes under low potential conditions and in the presence on CO and CO2. *Surf. Sci.* **2015**, *631*, 155-164.
(30) Chan, K. A few basic concepts in electrochemical carbon dioxide reduction. *Nat. Commun.* **2020**, *11* (1). DOI: 10.1038/s41467-020-19369-6.
(31) Nitopi, S.; Bertheussen, E.; Scott, S. B.; Liu, X.; Engstfeld, A. K.; Horch, S.; Seger, B.; Stephens, I. E.; Chan, K.; Hahn, C. Progress and perspectives of electrochemical CO2 reduction on copper in aqueous electrolyte. *Chem. Rev.* **2019**, *119* (12), 7610-7672.
(32) Hernandez-Aldave, S.; Andreoli, E. Fundamentals of gas diffusion electrodes and electrolysers for carbon dioxide utilisation: Challenges and opportunities. *Catal.* **2020**, *10* (6), 713.
(33) Ding, P.; An, H.; Zellner, P.; Guan, T.; Gao, J.; Müller-Buschbaum, P.; Weckhuysen, B. M.; van der Stam, W.; Sharp, I. D. Elucidating the Roles of Nafion/Solvent Formulations in Copper-Catalyzed CO2 Electrolysis. *ACS Catal.* **2023**, *13*, 5336-5347.
(34) Amiinu, I. S.; Li, W.; Wang, G.; Tu, Z.; Tang, H.; Pan, M.; Zhang, H. Toward anhydrous proton conductivity based on imidazole functionalized mesoporous silica/nafion composite membranes. *Electrochim. acta* **2015**, *160*, 185-194.

(35) Aldebert, P.; Dreyfus, B.; Gebel, G.; Nakamura, N.; Pineri, M.; Volino, F. Rod like micellar structures in perfluorinated ionomer solutions. *J. Phys.* **1988**, *49* (12), 2101-2109.
(36) Tarokh, A.; Karan, K.; Ponnurangam, S. Atomistic md study of nafion dispersions: Role of solvent and counterion in the aggregate structure, ionic clustering, and acid dissociation. *Macromolecules* **2019**, *53* (1), 288-301.
(37) Yamaguchi, M.; Matsunaga, T.; Amemiya, K.; Ohira, A.; Hasegawa, N.; Shinohara, K.; Ando, M.; Yoshida, T. Dispersion of rod-like particles of nafion in salt-free water/1-propanol and water/ethanol solutions. *J. Phys. Chem. B* **2014**, *118* (51), 14922-14928.
(38) Hölzle, M.; Zwing, V.; Kolb, D. The influence of steps on the deposition of Cu onto Au (111). *Electrochim. Acta* **1995**, *40* (10), 1237-1247.
(39) Uosaki, K.; Shen, Y.; Kondo, T. Preparation of a highly ordered Au (111) phase on a polycrystalline gold substrate by vacuum deposition and its characterization by XRD, GISXRD, STM/AFM, and electrochemical measurements. *J. Phys. Chem.* **1995**, *99* (38), 14117-14122.
(40) Magnussen, O.; Hotlos, J.; Beitel, G.; Kolb, D.; Behm, R. Atomic structure of ordered copper adlayers on single-crystalline gold electrodes. *J. Vac. Sci. Technol., B:Microelectron. Process. Phenom.* **1991**, *9* (2), 969-975.
(41) Xia, X.; Nagle, L.; Schuster, R.; Magnussen, O.; Behm, R. The kinetics of phase transitions in underpotentially deposited Cu adlayers on Au (111). *PCCP* **2000**, *2* (19), 4387-4392.
(42) Toney, M. F.; Howard, J. N.; Richer, J.; Borges, G. L.; Gordon, J. G.; Melroy, O. R.; Yee, D.; Sorensen, L. B. Electrochemical deposition of copper on a gold electrode in sulfuric acid: resolution of the interfacial structure. *Phys. Rev. Lett.* **1995**, *75* (24), 4472.
(43) Blum, L.; Huckaby, D. A.; Legault, M. Phase transitions at electrode interfaces. *Electrochim. Acta* **1996**, *41* (14), 2207-2227.
(44) Masuda, T.; Ikeda, K.; Uosaki, K. Potential-dependent adsorption/desorption behavior of perfluorosulfonated ionomer on a gold electrode surface studied by cyclic voltammetry, electrochemical quartz microbalance, and electrochemical atomic force microscopy. *Langmuir* **2013**, *29* (7), 2420-2426.
(45) Moffat, T. P.; Wheeler, D.; Josell, D. Electrodeposition of copper in the SPS-PEG-Cl additive system: I. kinetic measurements: Influence of SPS. *J. Electrochem. Soc.* **2004**, *151* (4), C262.
(46) Kuo, D.-Y.; Lu, X.; Hu, B.; Abruña, H. D.; Suntivich, J. Rate and Mechanism of Electrochemical Formation of Surface-Bound Hydrogen on Pt (111) Single Crystals. *J. Phys. Chem. Lett.* **2022**, *13* (27), 6383-6390.
(47) Lee, J. R.; O'Malley, R. L.; O'Connell, T. J.; Vollmer, A.; Rayment, T. X-ray absorption spectroscopy characterization of Cu underpotential deposition on Au (111) and organothiol-self-assembled-monolayer-modified Au (111) electrodes from sulfate supporting electrolyte. *J. Phys. Chem. C* **2009**, *113* (28), 12260-12271.
(48) Rousseau, B. J.; Lu, X.; Soudackov, A. V.; Suntivich, J.; Abruña, H.; Hammes-Schiffer, S. Theoretical Analysis of Hydrogen Underpotential Deposition on Pt (111) Under Alkaline Conditions. *J. Phys. Chem. C* **2024**, *128* (29), 12109-12120.
(49) Knöppel, J.; Möckl, M.; Escalera-López, D.; Stojanovski, K.; Bierling, M.; Böhm, T.; Thiele, S.; Rzepka, M.; Cherevko, S. On the limitations in assessing stability of oxygen evolution catalysts using aqueous model electrochemical cells. *Nat. Commun.* **2021**, *12* (1), 2231.
(50) Damjanovic, A.; Setty, T. H.; Bockris, J. M. Effect of crystal plane on the mechanism and the kinetics of copper electrocrystallization. *J. Electrochem. Soc.* **1966**, *113* (5), 429.
(51) Galus, Z. *Fundamentals of Electrochemical Analysis*; Ellis Horwood, 1991.

(52) Kang, R.; Zhao, Y.; Hait, D.; Gauthier, J. A.; Kempler, P. A.; Thurman, K. A.; Boettcher, S. W.; Head-Gordon, M. Understanding ion-transfer reactions in silver electrodissolution and electrodeposition from first-principles calculations and experiments. *Chem. Sci.* **2024**, *15* (13), 4996-5008.